J. Pharm. Pharmacol. 1983, 35: 133–137
Received September 21, 1982

0022–3573/83/030133–05 $02.50/0


# The influence of deposition method on the packing uniformity of powder beds

P. J. WOODHEAD* AND J. M. NEWTON**

* *Pharmacy Department, University of Nottingham, Nottingham NG7 2RD, and ** Pharmacy Department, Chelsea College, University of London, Manresa Road, London SW3 6LX, U.K.*

A number of methods of preparing powder packings have been assessed in terms of the resulting variability of local porosity. Measurement of local porosity was carried out by a γ-ray attenuation technique. It was found that overall porosity and the distribution of local porosity were highly dependent on particle properties and deposition method. Some deposition methods tended to give rise to the alternate formation and collapse of temporary structures within a growing bed, and in such cases, relatively high variability of local porosity was detected. More uniform packings could be formed by deposition of powder in even layers. In many cases, a significant relationship between local porosity and position within a packing was established, the central areas generally being of lowest porosity. This was true of packings both of high and low overall variability of porosity.

The bulk properties of a powder system are influenced by the way in which the individual particles pack together. One means of characterizing the structure of a powder bed is in terms of its porosity. In addition, there are instances in which uniformity of porosity is important, for example in minimizing the weight variation of tablets and dosator-filled hard gelatin capsules. A number of factors combine to determine the porosity of a powder packing. Some of these are the properties of the individual particles, such as their size, size distribution, shape and shape distribution, but also of importance is the method by which the particles are deposited to form a packing. Previous workers have demonstrated that the velocity and intensity of deposition are two of the most important factors affecting the overall porosity of a bed. Kolbuszewski (1950), studying sands, found that a low velocity of fall leads to a high porosity, irrespective of deposition intensity. A high velocity of fall was found to produce low porosity at low deposition intensities, but higher porosity at higher intensities. Macrae & Gray (1961) confirmed these findings in general, but observed that minimum porosity is achieved by maintaining the deposition intensity within certain limits. They concluded that a critical level of activity in the upper layers of a growing bed is necessary to enable particles to reach positions of least potential energy and closest packing. Eastwood et al (1969) evaluated a number of deposition methods in an effort to produce beds of high porosity. This was best achieved by rapid inversion of a cylindrical bed, thus providing high intensity and relatively low velocity of deposition.

* Present address: Glaxo Group Research, Ware, Herts.
** Correspondence.

The effect of deposition method on the variation of porosity within a powder bed was explored to some extent by van Brakel & Heertjes (1974). They employed an X-ray attenuation technique, in which local porosity is calculated from the observed attenuation of a narrow beam of X-radiation. Kurz & Schwedes (1976), on the other hand, chose a γ-ray attenuation method to measure the homogeneity of powder packings prepared for shear testing.

In a previous paper (Woodhead et al 1982), the development of a γ-ray technique for determining the distribution of local porosity in packings of lactose, was described in detail. The basis of the method is that if a powder sample of known thickness L is placed in the path of a narrow beam of γ-radiation, the observed count rate is reduced from $N_0$ to N, according to equation (1):

$$N = N_0 \exp[-\mu(1-\varepsilon)L] \qquad (1)$$

If μ, the linear attenuation coefficient of the sample material at the photon energy being used is known, then ε, the local porosity, can be calculated. The value of μ can be estimated from tables (Hubbell 1969) or determined experimentally using samples of known porosity.

The random nature of radioactive decay means that the precision of measurement of individual local porosity values can be improved by counting for longer time intervals. Using a statistical treatment established by Kurz (1972), it is possible to ensure that a local porosity value ε is measured with confidence intervals of $\pm\Delta\varepsilon$ at a probability level denoted by p. This is achieved by counting for sufficient time for the reference ('blank') count, $N_0$,

to exceed a minimum value, $N_{0_{min}}$, which is calculated from equation (2).

$$\frac{N_{0_{min}}}{p^2} = \left[\frac{\exp[-\frac{1}{2}\mu(1-\varepsilon-\Delta\varepsilon)L]+\exp[-\frac{1}{2}\mu(1-\varepsilon+\Delta\varepsilon)L]}{\exp[-\mu(1-\varepsilon-\Delta\varepsilon)L]-\exp[-\mu(1-\varepsilon+\varepsilon\Delta)L]}\right]^2 \quad (2)$$

The theoretical aspects of this technique, including the derivation of equation (2), appear in more detail elsewhere (Kurz 1972; Woodhead et al 1982), and will be applied in this work to evaluate the influence of method of powder deposition on the porosity variations within powder beds.

## MATERIALS AND METHODS

### *Materials and apparatus*

Crystalline lactose, in three particle size fractions, +18·7–26·5, +37·5–53 and +75–105 μm, was the particulate material used throughout. The powder was deposited into aluminium cylinders of depth 44 mm and internal diameter 19 mm. An aluminium extension tube of length 28 mm and internal diameter 19 mm enabled the containers to be overfilled; after removing the tube, the packing could then be levelled off.

The γ-ray attenuation system, described by Woodhead et al (1982), utilized a 200 mCi (7·4 GBq) sealed, directional point source of Americium-241, to direct a narrow cylindrical beam of 60 keV γ-radiation vertically through a prepared powder bed. Photons transmitted through the bed, i.e. not absorbed or scattered by the powder, were detected by a sodium iodide (thallium activated) crystal and recorded by a scaler-ratemeter (Ortec Ltd, Luton, Beds). Accurate positioning of the powder sample container was achieved by mounting it on a micromanipulator (Model 932/T, Prior, Bishops Stortford, Herts), itself firmly attached to the lead castle inside which the detector was housed.

### *Methods*

Five deposition methods were employed. In all cases, the extension tube was used to enable the containers to be overfilled. Levelling of the sample was carried out using a straight edge. The methods of filling are as follows:

1. Powder was poured directly from a jar into the cylinders.
2. Powder was allowed to discharge from a vertical cylindrical glass tube, of diameter 30 mm, through one of a number of interchangeable circular orifices of varying diameter, attached to the bottom of the tube. Deposition into a cylinder was only permitted during uninterrupted flow.
3. Powder was discharged from a vibrating chute of width 44 mm:

(i) through an aluminium funnel having an outlet of the same internal diameter as that of the cylinders.
(ii) through a steel plate in which a number of holes of 1·5 mm diameter had been drilled. The plate was of width 44 mm and was attached in such a way as to form an extension of the chute. The array of holes was devised by trial and error so that the vibration would cause powder to be deposited evenly over the whole cross-section of the cylinder positioned below.
(iii) into a cylinder placed on the rim of a turntable of 230 mm diameter. Manual oscillation of the turntable caused the cylinder to travel backwards and forwards through the plane of falling powder. In this way, the packing was built up in even layers.

In methods other than method 1, the vertical distance from the point at which the particles began free fall to the top of the cylinder was fixed at 100 mm. The corresponding distance for method 1 was not controlled, but was invariably less than 100 mm.

A number of preliminary runs were undertaken to establish the approximate rate of deposition into the containers of each particle size fraction, for each method used. It was not, however, possible to make such measurements for method 1.

Lactose packings for γ-ray attenuation measurements were prepared in lots of four. Each packing was weighed, and its overall porosity was calculated from the volume of the cylinder and the apparent particle density of lactose, previously determined to be 1·55 $g cm^{-3}$. The time interval for counting was determined from equation (2), into which the following values were substituted:

$p = 1{\cdot}96$ (95% confidence at ∞ degrees of freedom)
$\mu = 0{\cdot}288\ cm^{-1}$ (from tables (Hubbell 1969))
$\Delta\varepsilon = 0{\cdot}0050$

The values of L and ε were the measured thickness and overall porosity of the packing respectively. Local porosity determinations were carried out in each of 19 defined and evenly spaced positions by placing the container vertically in the radiation beam and counting for the required time interval. The reference count rate was recorded with an empty cylinder in the beam.

## RESULTS AND DISCUSSION

The observed rates of deposition for each particle size fraction and each deposition method are shown in Table 1. The +18·7–26·5 μm size fraction of lactose would not flow through any of the orifices available.

Table 1. Rates of deposition of powder samples

| Deposition method | Approximate rates of deposition (g min$^{-1}$) Size fractions of: +18·7–26·5 μm | +37·5–53 μm | +75–105 μm |
|---|---|---|---|
| 2(a)* | — | 630 | 290 |
| 2(b)* | — | 350 | 40 |
| 3(i) | 25 | 20 | 30 |
| 3(ii) | 5 | 15 | 20 |
| 3(iii) | 6 | 10 | 10 |

* Orifice diameters—
+37·5–53 μm fraction: (a) 15 mm, (b) 12 mm.
+ 75–105 μm fraction: (a) 9 mm, (b) 4 mm.

The calculation of individual local porosity values from γ-ray attenuation data required an accurate value for the linear attenuation coefficient, μ, of lactose. Previous experiments (Woodhead et al 1982) revealed this quantity to be dependent on porosity, and the following empirical expression was found to hold over the range of porosity encountered:

$$\mu_{lactose} = (0{\cdot}289 + 0{\cdot}0215\,\varepsilon)\ \text{cm}^{-1} \qquad (3)$$

Local porosities were calculated by an iteration performed by computer, beginning with a first approximation of $\mu = 0{\cdot}3\ \text{cm}^{-1}$. Alternate applications of equations (1) and (3) were repeated until successive approximations of local porosity differed by less than 0·0001. Values obtained in this way were translated into grey-scale images using a computer-controlled electrostatic printer. The 19 positions were represented by square regions, the darker areas being those of low porosity. Thus, for each particle size fraction and deposition method, 4×19 local porosity values were computed, enabling a group of four images to be produced.

The variability in local porosity was characterized using a statistical package (GENSTAT V). This included an analysis of variance on each group of four replicates of the 19 positions of measurement. Of these positions, one was at the centre of the packing, and there were six each at radial distances of 4, 7 and 8 mm from the centre. Pooling values at positions equidistant from the centre yielded a mean value for each radial distance. The analysis of variance revealed whether there was a significant relationship between porosity and radial position, whether such a relationship approximated to a linear, quadratic or cubic form, and whether there was a significant difference between samples. The grand mean of the 76 values gave a measure of the overall level of porosity, whilst minimum and maximum local values indicated the range present within a group of packings. A measure of overall variability was provided by the total sum of squares.

Table 2(a), (b) and (c) refer to the +18·7–26·5, +37·5–53 and +75–105 μm particle size fractions respectively. From these results, a number of observations can be made. The overall level of porosity was highest for the +18·7–26·5 μm size fraction and decreased with increasing particle size. This is as expected, since interparticulate forces increase in magnitude as particle size decreases, and particles are influenced less by gravitational forces. As a result, the particles are less likely to reach positions of minimum potential energy, i.e. closest packing.

All deposition methods employed a drop height of 100 mm (except method 1) hence for a given particle size fraction, velocity of deposition was not generally a variable. Deposition intensity, however, varied considerably with the method used. Method 3(iii), having the lowest deposition rate, gave the lowest porosity packings with all three particle size fractions. Methods 1 and 2, where applicable, produced packings of rather higher porosity, as a result of relatively high deposition intensity. Methods 3(i) and 3(ii), being of relatively low deposition intensity, would be expected to form low porosity beds. This was the case with the +75–105 μm beds, but the more cohesive size fractions did not follow the expected trend. Observation of these beds during deposition revealed that a number of discrete heaps of powder tended to alternately build up and collapse due to cohesion between particles. Thus, much of the powder was being redeposited at a velocity lower than the original incident velocity. In addition a relatively cohesive material such as +18·7–26·5 μm lactose tends to be deposited as agglomerates rather than independent particles.

Methods 3(i) and 3(ii) also produced packings of high variability of porosity, as represented by 'total sum of squares', for possibly the same reasons as they gave packings of higher porosity than anticipated. Method 3(iii), which built packings layer by layer, generally produced the most uniform beds, although methods 1 and 2 also resulted in relatively low variability of porosity. A comparison of Figs 1 and 2 illustrates, for +37·5–53μm lactose, that discharge from a cylindrical tube through a 15 mm diameter orifice results in more uniform packing than discharge from a vibrating chute via a funnel.

Table 2. Statistical analysis of local porosity in packings of lactose of particle size (a) 18·7–26·5 μm (b) 37·5–53 μm (c) 75–105 μm, prepared by different methods.

| (a) Filling method | 1 | 3(i) | 3(ii) | 3(iii) |
|---|---|---|---|---|
| Grand mean porosity | 0·670 | 0·690 | 0·666 | 0·625 |
| Minimum local value | 0·650 | 0·628 | 0·631 | 0·606 |
| Maximum local value | 0·699 | 0·750 | 0·722 | 0·656 |
| Mean local porosity | | | | |
| r = 0 mm | 0·662 | 0·652 | 0·682 | 0·616 |
| r = 4 mm | 0·665 | 0·673 | 0·640 | 0·621 |
| r = 7 mm | 0·671 | 0·697 | 0·668 | 0·624 |
| r = 8 mm | 0·675 | 0·706 | 0·686 | 0·631 |
| Variance ratios: | | | | |
| Distance from centre | 4·903** | 9·575** | 29·271** | 9·691** |
| Linear fit | 14·258** | 24·248** | 61·932** | 17·538** |
| Quadratic fit | 0·414 | 4·169* | 0·213 | 0·133 |
| Cubic fit | 0·038 | 0·309 | 25·666** | 1·402 |
| Between samples | 4·150** | 0·143 | 0·446 | 8·935** |
| Total sum of squares | 0·00949 | 0·0685 | 0·0500 | 0·00618 |

| (b) Filling method | 1 | 2a† | 2b‡ | 3(i) | 3(ii) | 3(iii) |
|---|---|---|---|---|---|---|
| Grand mean porosity | 0·565 | 0·538 | 0·526 | 0·536 | 0·550 | 0·499 |
| Minimum local value | 0·536 | 0·512 | 0·508 | 0·453 | 0·504 | 0·481 |
| Maximum local value | 0·592 | 0·561 | 0·549 | 0·586 | 0·581 | 0·522 |
| Mean local porosity | | | | | | |
| r = 0 mm | 0·555 | 0·527 | 0·511 | 0·539 | 0·529 | 0·497 |
| r = 4 mm | 0·562 | 0·532 | 0·518 | 0·524 | 0·549 | 0·501 |
| r = 7 mm | 0·567 | 0·539 | 0·529 | 0·537 | 0·554 | 0·495 |
| r = 8 mm | 0·568 | 0·544 | 0·535 | 0·548 | 0·551 | 0·501 |
| Variance ratios: | | | | | | |
| Distance from centre | 1·537 | 10·981** | 39·207** | 2·685 | 3·528* | 2·750 |
| Linear fit | 3·348 | 30·387** | 109·547** | 7·086* | 2·056 | 0·267 |
| Quadratic fit | 1·030 | 2·441 | 7·895** | 0·111 | 4·672* | 5·555* |
| Cubic fit | 0·234 | 0·116 | 0·182 | 0·857 | 3·857 | 2·427 |
| Between samples | 2·764* | 25·168** | 5·956** | 0·082 | 4·422** | 1·356 |
| Total sum of squares | 0·0172 | 0·0118 | 0·00792 | 0·09 | 0·0186 | 0·00592 |

| (c) Filling method | 1 | 2a | 2b | 3(i) | 3(ii) | 3(iii) |
|---|---|---|---|---|---|---|
| Grand mean porosity | 0·523 | 0·515 | 0·530 | 0·478 | 0·474 | 0·446 |
| Minimum local value | 0·500 | 0·494 | 0·509 | 0·421 | 0·429 | 0·424 |
| Maximum local value | 0·543 | 0·530 | 0·545 | 0·512 | 0·513 | 0·478 |
| Mean local porosity | | | | | | |
| r = 0 mm | 0·516 | 0·505 | 0·514 | 0·468 | 0·483 | 0·434 |
| r = 4 mm | 0·518 | 0·507 | 0·527 | 0·480 | 0·482 | 0·439 |
| r = 7 m | 0·524 | 0·518 | 0·534 | 0·479 | 0·472 | 0·444 |
| r = 8 mm | 0·526 | 0·521 | 0·533 | 0·475 | 0·465 | 0·457 |
| Variance ratios: | | | | | | |
| Distance from centre | 3·973* | 45·342** | 30·637** | 0·279 | 3·832* | 16·101** |
| Linear fit | 10·122** | 120·462** | 49·536** | 1·125 | 11·139** | 47·255** |
| Quadratic fit | 1·789 | 14·701** | 31·437** | 0·332 | 0·289 | 0·589 |
| Cubic fit | 0·008 | 0·864 | 10·939** | 0·379 | 0·069 | 0·460 |
| Between samples | 4·984** | 4·072* | 2·567 | 0·025 | 1·189 | 1·011 |
| Total sum of squares | 0·00747 | 0·00505 | 0·00362 | 0·0486 | 0·0277 | 0·0116 |

a = 9 mm orifice; † 15 mm. * Significant at the 5% level of probability.
b = 4 mm orifice; ‡ 12 mm. ** Significant at the 1% level of probability.

The analysis of variance revealed that in many cases, a significant relationship between local porosity and radial position exists. Fig. 3, which represents packings of +75–105 μm lactose deposited from a cylindrical tube through a 4 mm orifice, is an example wherein the central regions are of lower porosity than the outer regions. In this instance, the low porosity in the centre of the packings coincides with the area in which most particles were initially deposited. However, a similar effect is generally observed with method 3(iii) in which steps were taken to deposit powder evenly over the whole cross-section of each packing.

The incidence of a significant difference between

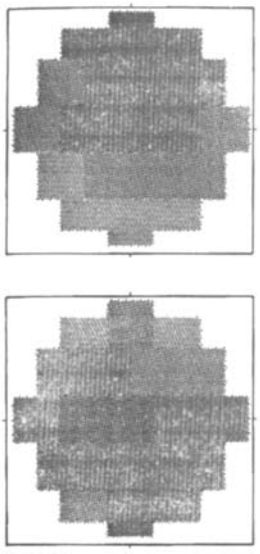

FIG. 1. Grey-scale images, illustrating radial porosity variations in samples of lactose, size fraction +37·5–53 μm, deposited from a vertical glass tube fitted with a 15 mm diameter orifice. Mid-range porosity 0·536; porosity increment 0·01.

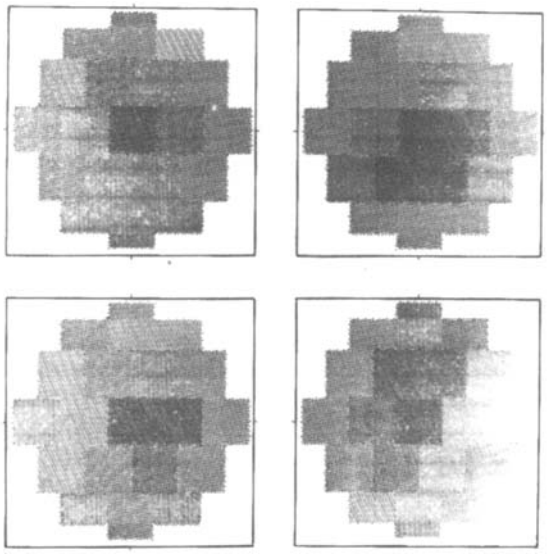

FIG. 3. Grey-scale images, illustrating radial porosity variations in samples of lactose, size fraction +75–105 μm, deposited from a vertical glass tube fitted with a 4 mm diameter orifice. Mid-range porosity 0·527; porosity increment 0·005.

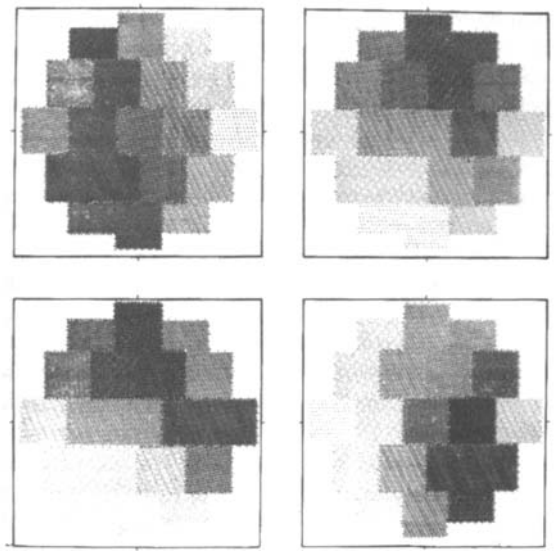

FIG. 2. Grey-scale images, illustrating radial porosity variations in samples of lactose, size fraction +37·5–53 μm, deposited from a vibrating chute and funnel. Mid-range porosity 0·519; porosity increment 0·01.

samples in a group of four did not follow any clear trend, although methods producing high overall variability of porosity, such as method 3(i), generally failed to show a significant between-samples variance ratio.

In conclusion, these experiments have shown that the degree of uniformity of a powder packing depends not only on the properties of the particulate material, but on the method of preparation of the packing. The results have illustrated some of the concepts of previous workers, but have shown that cohesive properties have an influence on the way particles pack.

## REFERENCES


Eastwood, J., Matzen, E. J. P., Young, M. J., Epstein, N. (1969) Br. Chem. Eng. 14: 1542–1545

Hubbell, J. H. (1969) National Bureau of Standards Report, NSRDS–NBS 29, Photon cross sections

Kolbuszewski, J. (1950) Research (London) 3: 478–483

Kurz, H. P. (1972) Powder Technol. 6: 167–170

Kurz, H. P., Schwedes, J. (1976) Chemi-Eng.-Technol. 48: 555

Macrae, J. C., Gray, W. A. (1961) Br. J. Appl. Phys. 12: 164–172

van Brakel, J., Heertjes, P. M. (1974) Powder Technol. 9: 263–271

Woodhead, P. J., Hardy, J. G., Newton, J. M. (1982) J. Pharm. Pharmacol. 34: 352–358